Solution Structure of the Parallel-Stranded Hairpin d(T8⟨⟩C4A8) As Determined by Two-Dimensional NMR†

Ning Zhou,‡ Markus W. Germann,‡ Johan H. van de Sande,§ N. Pattabiraman,∥,⊥ and Hans J. Vogel*,‡

Departments of Biological Sciences and Medical Biochemistry, University of Calgary, Calgary, Alberta T2N 1N4, Canada, and Laboratory for the Structure of Matter, Naval Research Laboratory, Washington, D.C. 20375

Received July 2, 1992; Revised Manuscript Received October 30, 1992

ABSTRACT: The structure of the oligodeoxynucleotide (3′)T8(5′)–(5′)C4A8(3′) hairpin in aqueous solution was studied by two-dimensional (2D) proton and phosphorus nuclear magnetic resonance (NMR) spectroscopy. At 2.5 mM and 10 °C, the molecule exists predominantly as a monomolecular hairpin with a C4 loop. At higher concentrations and lower temperatures, NMR signals from multimers are obvious. They account for ~25% of the total population at 4 mM and 10 °C. Nearly all of the proton NMR signals for the hairpin could be assigned using 2D COSY, HOHAHA, and NOESY experiments. 2D ^{1}H–^{31}P correlation experiments were used to assign all the phosphorus resonances and to provide an additional check for the sequential assignments. A parallel-stranded T8·A8 stem can be formed in the hairpin due to the presence of the unusual 5′–5′ linkage in the loop. 2D NOESY experiments indicate that the A H2 and its 5′-end neighbor base pair T methyl protons are within 5 Å of each other. This is in accord with reverse Watson–Crick base pairing between T and A, which locates the A H2 and the T methyl protons in the same groove of the duplex. The chemical shifts of A H1′, H2′, and H2″ sugar and the H2 base protons are quite different compared to normal B-DNA. Analysis of the 2D COSY and NOESY cross peak patterns indicates that the deoxyribose rings are mainly in the C2′-endo conformation and that the stem forms a right-handed helix, with the two strands held together by eight reverse Watson–Crick A·T base pairs to form a parallel-stranded duplex. The backbone torsion angles, as determined from the ^{31}P chemical shifts, are slightly different for the A and the T residues. A molecular model was constructed, using a total of 336 proton NOE cross peak intensities as proton–proton distance constraints. In the refined structure, the conformations of the sugar–phosphate linkage, the deoxyribose rings, and the glycosyl bonds for the two parallel strands of the hairpin are close to a regular B-DNA structure. The base-stacking and the hydrogen-bonding interactions are well optimized; however, the two grooves are of approximately equal width. Thus, compared to B-DNA, the parallel-stranded duplex has a very different surface shape, and because of the reverse Watson–Crick base pairing, it has different groups exposed in each groove.

A common feature of A-, B-, and Z-DNA duplexes is the antiparallel orientation of the constituent strands. However, a number of studies have shown that the formation of a parallel-stranded duplex, in which both sugar–phosphate strands run in the same direction, is feasible. Its formation can be promoted through the use of modified oligonucleotides. For example, α-deoxyoligonucleotides and the complementary β-deoxyoligonucleotides (Morvan et al., 1987; Thuong et al., 1987; Praseuth et al., 1987), as well as deoxyoligonucleotides that contain methylated phosphate triesters (Koole et al., 1987; Quaedflieg et al., 1990) can form a parallel structure. The stabilization of a parallel-stranded double-helical structure in natural oligodeoxynucleotides has also been accomplished by applying extreme conditions, such as low pH which leads to the protonation of C or A base (Sarma et al., 1986; Sanger, 1984). Furthermore, cationic oligopeptides can induce the formation of a parallel duplex in the natural oligomer dT_{10} (van Genderen et al., 1990). However, in all these cases, the formation of the parallel structure is a consequence of unusual features that are not normally present in natural DNA. We have studied parallel-stranded duplex formation at neutral pH by natural oligodeoxyribonucleotides containing homo-oligomeric A·T sequences or alternating d(A·T) segments (van de Sande et al., 1988; Germann et al., 1988, 1989, 1990). This earlier work, as well as the studies by Jovin and co-workers (Ramsing & Jovin, 1988; Ramsing et al., 1989; Rippe et al., 1989; Otto et al., 1991), have provided evidence that parallel-stranded DNA formation is not restricted to modified nucleotides or to extreme conditions but that it can occur in normal AT-rich DNA with appropriate sequence homology. Molecular mechanics calculations of homooligomeric dA·dT duplexes (Pattabiraman, 1986) have shown that a parallel-stranded right-handed double helix with reverse Watson–Crick base pairing between A and T is energetically almost equally as favorable as the conventional antiparallel structure with regular Watson–Crick base pairing. In the calculated structure, each strand of the parallel-stranded duplex remains very similar to that of regular B-DNA. In the present study, we have used high-resolution two-dimensional proton–proton and proton–phosphorus NMR[1] to further define the three-dimensional structure of the parallel-stranded DNA hairpin d(T8⟨⟩C4A8). Proton NOE data provided unambiguous

† This work was supported by the Medical Research Council (MRC) of Canada. The NMR spectrometers were purchased through grants from MRC and AHFMR (Alberta Heritage Foundation for Medical Research). The molecular graphics computer and software were obtained with financial aid from the Hasselblad Foundation. H.J.V. is an AHFMR scholar.

* To whom correspondence should be addressed.
‡ Department of Biological Sciences, University of Calgary.
§ Department of Medicinal Biochemistry, University of Calgary.
∥ Naval Research Laboratory.
⊥ Permanent address: GEO Centers, Inc., 10903 Indian Head Highway, Fort Washington, MD 20744.

[1] Abbreviations: COSY, 2D correlated spectroscopy; DQF, double-quantum filtered; HOHAHA, 2D homonuclear Hartman–Hahn spectroscopy; NMR, nuclear magnetic resonance; NOE, nuclear Overhauser effect; NOESY, 2D NOE spectroscopy; rmsd, root-mean-square deviation.

0006-2960/93/0432-646$04.00/0

evidence for the existence of reverse Watson–Crick base pairing between A and T. Information about sugar ring puckering, base orientation, and the backbone conformation was obtained, and an NOE-restrained energy-minimized model was calculated which reveals the detailed structure of the parallel-stranded hairpin.

METHODS AND MATERIALS

The oligonucleotide d(T8⟨⟩C4A8) was synthesized as described previously (Germann et al., 1989). The concentration of the samples used for the NMR study was 2.5 mM unless otherwise stated. Samples were made up in aqueous 10 mM phosphate buffer solution (pH 7.0) containing 0.1 M NaCl and 0.1 mM EDTA. Before the NMR measurements, the samples were lyophilized several times from pure D_2O.

The NMR measurements were carried out on a Bruker AM-400 wide-bore spectrometer equipped with an Aspect-3000 computer and on a Bruker AMX-500 spectrometer equipped with an X-32 computer. Pure-absorption phase 2D spectra were obtained using the time-proportional phase incremental method (TPPI) (Marion & Wüthrich, 1983). For all experiments, the carrier frequency was set at the residual HDO peak. The NOESY experiments were acquired with mixing times of 25, 40, 62.5, 90, 125, and 250 ms; the pulse repetition time was 3.2 s. The mixing times were randomly varied within a range of 5% to suppress zero-quantum effects as proposed by Macura et al. (1981). This scheme appeared to be sufficient; no out-of-phase peaks were detected for any of the sugar protons. Moreover, "positive" and "positive plus negative" intensities of some of the cross peaks were integrated and proved to be essentially identical (agree within 2% to each other), which further indicated that zero-quantum effects were negligible. A recent study (Wang et al., 1992) has also shown that the influence of zero-quantum effects on NOESY cross peak is negligible. The experimental temperature was 10 °C unless otherwise stated. A total of 512 FIDs of 2K size with 48 scans each were collected, and 45°-shifted sine-bell multiplication and zero-filling were applied in both dimensions before Fourier transformation. HOHAHA experiments were obtained using MLEV-17 spin-locking pulses and isotropic mixing times of 67 and 250 ms (Bax & Davis, 1985). Data size and processing parameters were similar to those used in the NOESY experiments. DQF-COSY spectra (Rance et al., 1983) were obtained at both 10 and 20 °C. A total of 800 FIDs of 4K size were collected with 48 scans of each. Irradiation of the residual HDO peak was used to reduced its intensity. The pulse repetition time was 2 s. Similar processing parameters were used as for the NOESY spectra except that the final data set size was larger (4K × 2K). This yields a resolution of 1.2 Hz/point in the t_2 dimension and of 2.4 Hz/point in the t_1 dimension. The phosphate-decoupled DQF-COSY spectrum was measured using an inverse probe head, with phosphorus broad-band decoupling during acquisition. All the other parameters were the same as for the DQF-COSY experiments. The time for collecting each 2D experiment varied between 18 and 22 h.

The 2D ^1H–^{31}P correlation experiment was recorded at a ^1H frequency of 500 MHz with ^1H detection; the ^1H signal was presaturated with a train of 40 180° pulses (spaced by 50 ms) during the delay time between consecutive scans (Sklenar et al., 1986). Sweep widths in F_2 (^1H) and F_1 (^{31}P) dimensions are 8 and 4 ppm, respectively. A total of 128 2K size FIDs were collected with 128 scans each. Zero-filling and sine-bell multiplication was used in both dimensions before Fourier transformation to get the final spectra. Phosphorus chemical shifts are reported relative to external phosphoric acid (85%) at 0.0 ppm.

MIDAS (Computer Graphics Laboratory, University of California, San Francisco) and AMBER (Singh et al., 1988) programs were used to build the starting molecular model. The coordinates of double-helical structures for the sequences T8 (referred as T-strand) and C4A8 (referred as A-strand) were generated from the B-DNA coordinates reported by Arnott and Hukins (1972) Only the coordinates of the strand containing the above-mentioned sequences of the duplex were extracted such that the sugar–phosphate chain of the A nucleotides are superimposed on the sugar–phosphate chain of the T nucleotides. As described earlier (Pattabiraman, 1986), the coordinates of the A-strand were rotated about the z- (or helix) axis by ~190° in order to form two reasonable hydrogen bonds between atoms N6 and N1 of A and O_4 and N_3 of T, respectively. Thus all adenine bases form a reverse Watson–Crick base pair with the corresponding thymine bases. In addition, the two sugar–phosphate chains are parallel in their orientation. All hydrogen atoms were modeled explicitly.

Visual model building of the loop containing cytosine nucleotides were carried out by changing backbone and glycosyl torsion angles of C residues such that the free 5′-end oxygen of the C in the A-strand forms a bond with the atom P of the 5′-end residue in the T-strand, and reasonable stereochemistry around this bond is retained. By treating the unusual 5′–P–5′ linkage in a manner similar to disulfide linkages in proteins, the program AMBER (as well as XPLOR, see below) can be used without further modification.

NOE cross peaks from NOESY experiments were categorized as "weak", "medium", and "strong" according to their intensities measured in a 125-ms NOESY spectrum as described elsewhere (Zhou & Vogel, 1993). These were converted to the following approximate proton–proton distance restraints: weak, ≤5.0 Å; medium, ≤3.6 Å; strong, ≤2.8 Å, with a lower limit of 2 Å for all three groups (Bax, 1989). These constraints were used in a molecular mechanics calculation. Other weak NOE cross peaks, which could only be observed with longer mixing times (>125 ms), were useful for making assignments, but they were not used as constraints because increasing spin–diffusion at longer mixing times can lead to erroneous results. The NOEs involving methyl protons and intraresidue NOEs involving H5′ and H5″ protons were also not used. This is because the stereospecific assignments of the H5′ and H5″ protons were not available, and extra motions of the methyl protons might complicate the interpretation of their NOEs.

The software package QUANTA/XPLOR (Polygen Corporation), which was run on a Silicon Graphics IRIS 4D/25 computer, was used to refine the molecular model. The empirical energy functions developed by Nilsson and Karplus (1986) for DNA were used with explicit hydrogen-bond potential. NOE constraints were incorporated as a square-well pseudo-energy term $E_{NOE} = \sum K_b T S \Delta^2$, where K_b is the Boltzmann constant, T is the temperature, S is a scale factor assigned to be 30, and Δ is a value determined for the NOE constraint. A dielectric constant proportional to distance (Brooks et al., 1983) was used in calculating the electrostatic potential to mimic solvent effects. A nonbonded interaction cutoff distance of 11.5 Å was used with a cubic switching function between 9.5 and 10.5 Å. Energy minimization with the Powell algorithm (Powell, 1977) was carried out until the energy change was smaller than 0.1 kcal/Å.

RESULTS AND DISCUSSION

The partly self-complementary DNA oligonucleotide d(T8⟨⟩C4A8) contains a 5′–P–5′ phosphodiester linkage, which is not a normal linkage in DNA or RNA. This unusual linkage was introduced in the loop to promote the formation of a parallel-stranded hairpin. Since the unusual linkage is located in the loop, it does not introduce any unusual features in the stem part.

Equilibrium between Parallel-Stranded Hairpin and Other Forms. We have shown previously (Germann et al., 1989) that the oligonucleotide d(T8⟨⟩C4A8) in aqueous solution is engaged in a concentration- and temperature-dependent conformational equilibrium. This polymorphic behavior was studied here in more detail in order to establish conditions for NMR experiments under which the parallel-stranded hairpin form is dominant. The concentration- and temperature-dependent formation of the multimeric form (resonances marked with an asterisk) is shown in Figure 1. A significant amount of the multimer(s) was observed for the sample with 4 mM strand concentration at 10 °C, and it increases even further at lower temperatures. In contrast, the sample is predominantly in a monomolecular hairpin conformation at 2.5 mM strand concentration and 10 °C (Figure 1). Consequently, we have performed all our 2D experiments at 10 °C and 2.5 mM. The pronounced concentration dependence that was observed for the formation of the multimeric structure argues against the presence of dimers, and our data suggest that the multimeric structures consist of more than four oligonucleotides. Exchange peaks between the hairpin and the multimeric forms were observed for the 4 mM sample in 2D NOESY experiments.

Base Pairing. Eight proton resonances in the 7.2–7.8 ppm region are characterized by a narrower line width and a longer spin–lattice relaxation times (T_1) compared with the other aromatic proton resonances. Their T_1 values range from 2.00 to 2.55 s (±0.05), while all other aromatic proton T_1's are shorter than 2 s. These protons display detectable NOEs with each other (Figure 2) but not to any sugar H2′, H2″, or H3′ protons; in addition, only very weak NOEs to sugar H1′ protons are observed (see below). This pattern is quite different from the NOE pattern displayed by base H6 and H8 protons and indicates that these resonances are the base H2 protons of the A residues (Wüthrich, 1986). Interstrand NOE cross peaks between the A H2 protons and T methyl protons were observed in the NOESY spectra (Figure 3). Such NOEs are not observed for a normal B-type DNA duplex which is held together by Watson-Crick base pairing (Scheek et al., 1983, 1984). In regular B-DNA, the T methyl group is located in the major groove of the duplex, while the A H2 is in the minor groove at the opposite side of the duplex (Chart I). The A H2 to T CH_3 NOEs are also not consistent with the presence of Hoogsteen base pairs. In the Hoogsteen base pair scheme, the T methyl and the A H2 are again more than 5 Å apart, and hence they would not give rise to a cross peak in a NOESY spectrum. However, in reverse Watson–Crick A·T base pairs, the T methyl groups are brought into the same groove as the A H2 protons (Chart I). The distance from the A H2 to the T methyl protons of the same base pair and to the T methyl protons of the 5′-end T in the neighboring base pair are now reduced to less than 5 Å. Thus, the observed NOE interactions between A H2 and T methyl protons are characteristic of the formation of reverse Watson–Crick base pairs between A and T residues. It is noteworthy that this NOE interaction has not been reported before for any other DNA structure (Cohen, 1987).

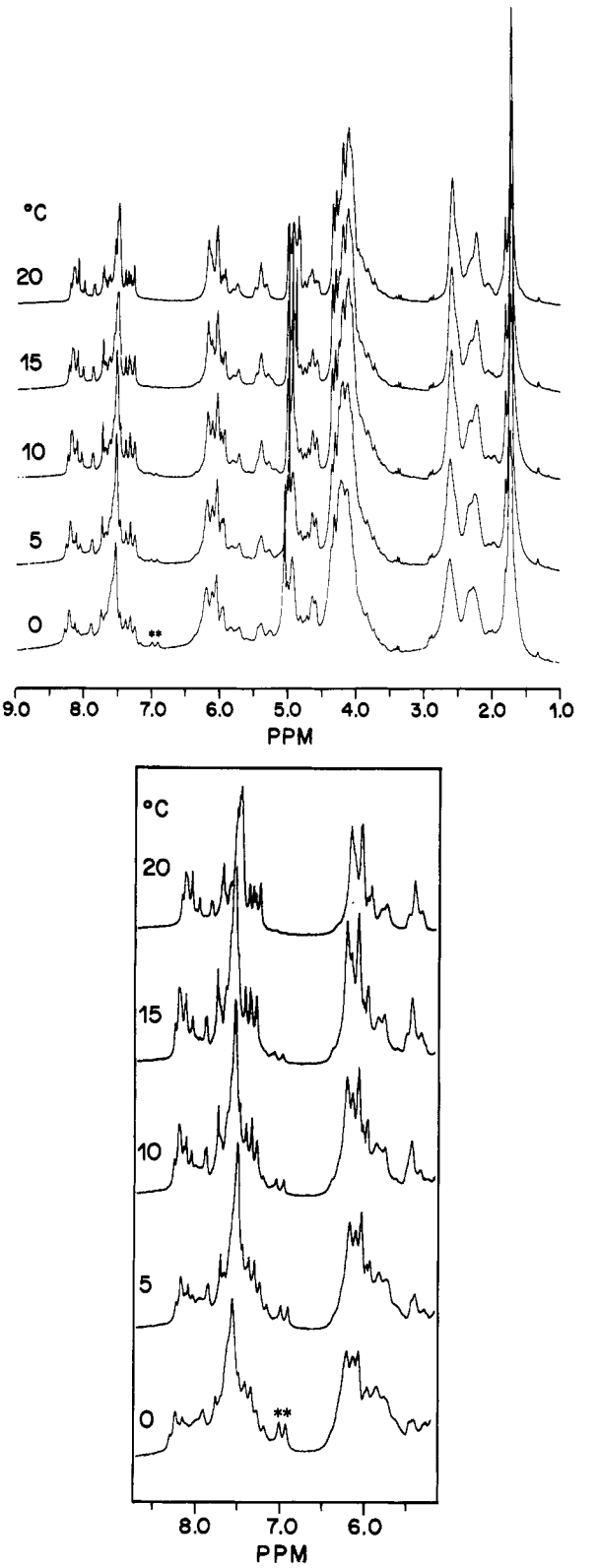

FIGURE 1: Proton NMR spectra (400 MHz) of the d(T8⟨⟩C4A8) hairpin at 2.5 mM (upper panel) and 4 mM (lower panel) concentration recorded at the different temperatures as indicated. The peaks marked with an asterisk in the spectra recorded at 0 °C arise from the multimer. They decrease in intensity when the temperature is raised (see the text for details).

Proton Resonance Assignments. As a first step toward the complete assignment of the proton NMR spectrum, the deoxyribose proton resonances from each residue were identified with the help of HOHAHA experiments. In the spectrum recorded with an isotropic mixing time of 67 ms

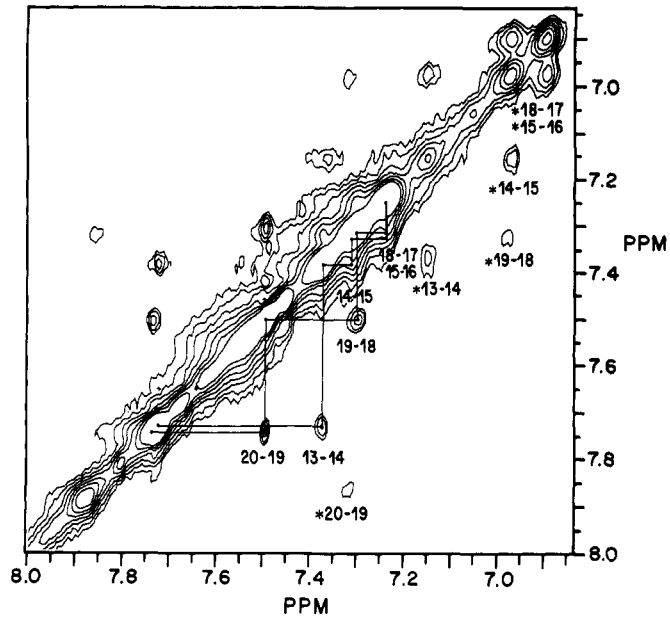

FIGURE 2: Region of the NOESY spectrum of 4 mM d(T8⟨⟩C4A8), recorded with a mixing time of 250 ms, showing the cross peaks between the aromatic A H2 protons from the parallel-stranded hairpin form and from the multimeric (*) antiparallel form(s). The cross peaks are labeled with the two residue numbers of the A H2 protons that they connect (see Chart II for numbering system). Experimental details are given under Methods and Materials.

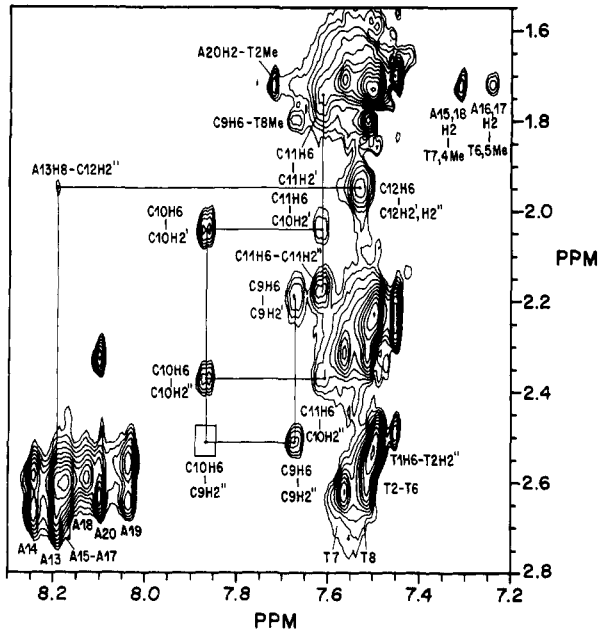

FIGURE 3: Aromatic proton–H2", methyl (Me) proton region of a 500-MHz NOESY spectrum of d(T8⟨⟩C4A8) (2.5 mM) recorded with a mixing time of 250 ms. In addition to the intraresidue H8-(H6)–H2', H8(H6)–H2", and interresidue (i+1)H8(H6)–(i)H2" cross peaks, several interstrand NOE cross peaks between AH2(i) and TMe(22–i) are also labeled.

(Figure 4), cross peaks between sugar protons of the same nucleotide were detected for three groups of protons: (1) H1', H2', H2", and H3'; (2) H3' and H4'; and (3) H4', H5', and H5" protons. With this isotropic mixing time, no multiple-step magnetization transfer was observed across the H3'–H4' coupling. However, the entire spin system of the deoxyribose could be correlated in a HOHAHA experiment recorded with a longer isotropic mixing time (250 ms). Base protons from C, T, and A residues were distinguished on the basis of their different cross peak patterns in the HOHAHA experiments. The C base protons H6 and H5 were readily identified by a

Chart I: Comparison of the Watson–Crick (Top) and the Reverse Watson–Crick A·T Base Pairing (Bottom)[a]

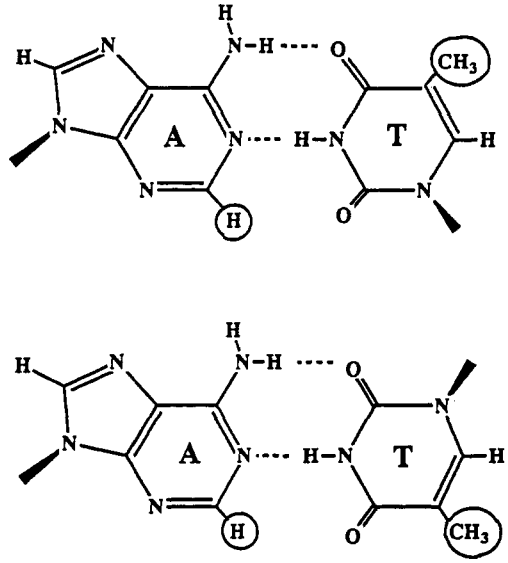

[a] The A H2 and the T methyl protons are circled. They are located in different grooves with Watson–Crick base pair scheme, but in the same groove with reverse Watson–Crick base pairing scheme.

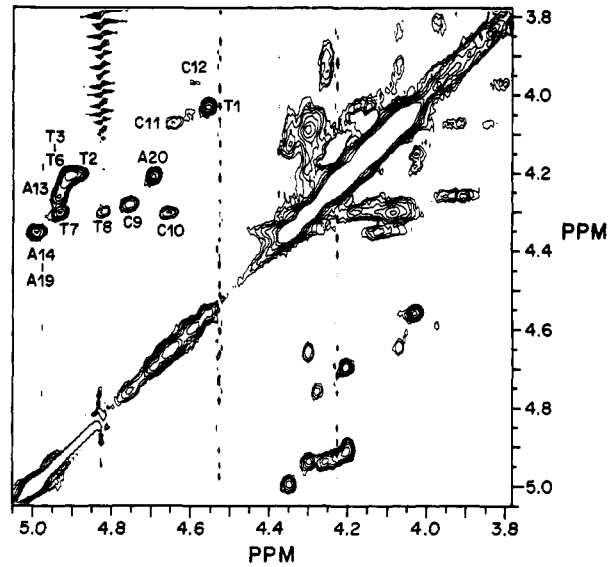

FIGURE 4: Expansion of the H3'–H4', H5', H5" proton region of a 400-MHz HOHAHA spectrum of d(T8⟨⟩C4A8), recorded with an isotropic mixing time of 67 ms. The H3'–H4' cross peak of each residue is labeled with the appropriate residue name.

strong cross peak in the downfield area, while each of the T H6 proton gave a weak cross peak to an upfield methyl proton resonance (data not shown). The remainder of the resonances in the aromatic region were from A H8 and A H2 protons. The A H2 protons were distinguished by their longer T_1 values and distinct NOE patterns (see above), and thus the A H8 protons were identified by elimination. In addition to the one-dimensional NOE results that we published earlier for this hairpin (Germann et al., 1989), we have also recorded 2D NOESY experiments in H_2O/D_2O solution and observed NOEs between the imino and the A H2 protons. This is as expected for reverse Watson–Crick base pairing. This experiment, however, did not provide information about sequence-specific assignments of the A H2 protons due to the poor resolution of the imino proton signals [see Figure 8 in Germann et al. (1989)]. Our data show that the proton resonances of the parallel-stranded hairpin molecule fall

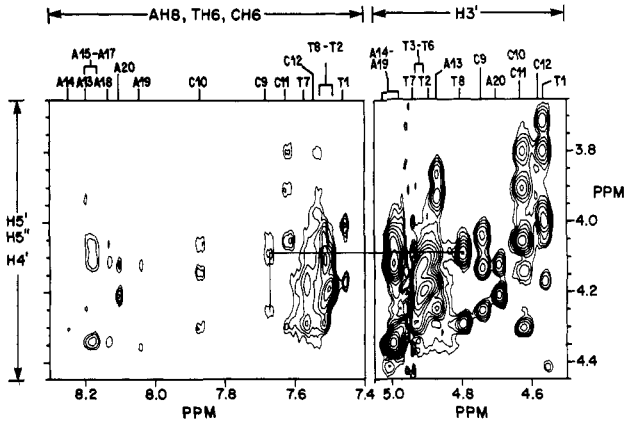

FIGURE 5: Two regions of the 500-MHz NOESY spectrum of d(T8⟨⟩C4A8) (2.5 mM) recorded with a mixing time of 250 ms. Shown in the left panel are the intraresidue NOE cross peaks between the aromatic proton and the H4′, H5′, and H5″ protons. The intraresidue cross peaks between the H3′ and H4′, H5′, and H5″ protons are shown in the right panel. The unique interresidue C9 H6–T8 H5′, H5″ cross peaks are indicated by lines. The labels on the top give the assignments of the H8(H6) protons (left panel) and the H3′ (right panel) protons.

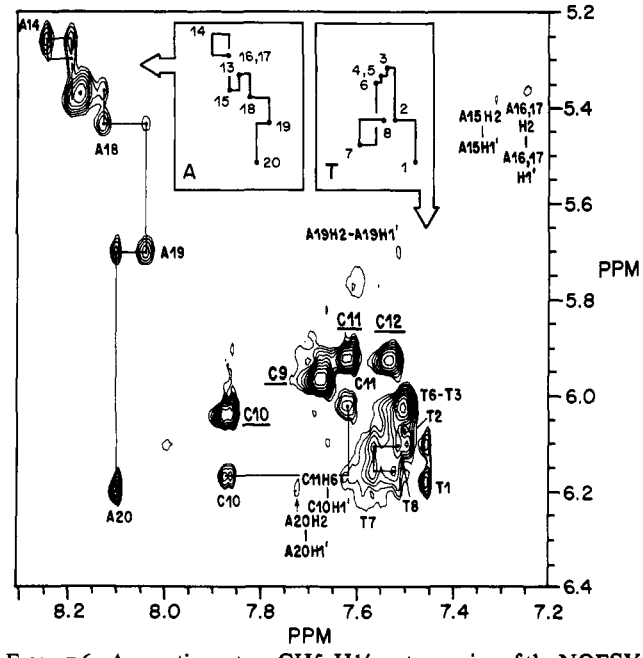

FIGURE 6: Aromatic proton–CH5, H1′ proton region of the NOESY spectrum as described in the legend of Figure 3. The strong C H6–H5 cross peaks are labeled with underlined residue names. The sequential connections of H8(H6) to its 5′-end H1′ cross peak for the T- and the A-strands are depicted in the two boxes. Also labeled are the connections between residues C10 and C11, as well as the weak intraresidue NOEs of A H2–A H1′.

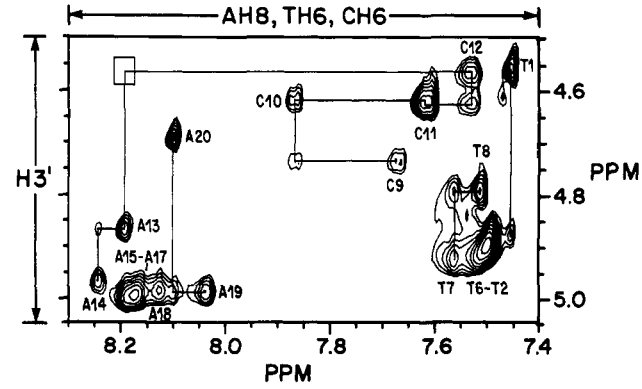

FIGURE 7: Aromatic proton–H3′ proton region of the NOESY spectrum as described in the legend of Figure 3. The intraresidue H8(H6)–H3′ cross peaks are labeled with the residue name, and interresidue cross peaks are linked to them by lines. The interresidue H6(*i*)–H3′(*i*–1) cross peaks of the C residues are well resolved and are used to make their sequential assignments. A weak NOE between A13 H8 and C12 H3′ was only visible at a lower contour level and is indicated in the plot by a box.

roughly in the same chemical shift ranges as those of the same type of protons in normal duplexes [for a review, see van de Ven and Hilbers (1988)] or in antiparallel-stranded hairpins [see, for example, Blommers et al. (1991) and Zhou and Vogel (1993)]. For instance, the purine A H8 proton resonances are in the most downfield area (around 8 ppm), and the pyrimidine H6 protons and the A H2 protons are found in the 7.2–7.9 ppm range. The majority of the A H1′ proton resonances are in the range of 5.2–5.4 ppm; these are about 0.4 ppm upfield-shifted compared to the A H1′ protons of the related antiparallel hairpin d(T8C4A8) (Zhou & Vogel, 1993). These are the most noticeable chemical shift differences between the corresponding protons of the two molecules.

The base and sugar protons are not scalar coupled, and no scalar coupling between the protons in neighboring residues exists; therefore, NOESY spectra, rather than HOHAHA or DQF-COSY spectra, were used to make the sequential assignments. The unusual structure of the molecule provided several starting points for making the assignments. For example, when the sample temperature was increased toward the melting point, resonances of one T residue and one A residue shifted significantly, indicating that they are at end positions. In addition, their H3′ protons were found about 0.3 ppm upfield from the other T H3′ and A H3′ protons (Figure 4). Thus, we assigned these to the T1 H3′ and A20 H3′, which both lack a 3′-phosphate group and therefore display distinct H3′ proton chemical shifts. Secondly, unique interresidue NOE cross peaks between one of the C H6 protons and the H5′ and H5″ protons of one T residue were detected (Figure 5). This interaction is only likely to occur between T8 and C9, because of the presence of the unusual 5′–5′ phosphodiester linkage. Therefore, these two residues were assigned accordingly. It is known that the intraresidue proton distance H8–H1′ (and H6–H1′) is under 4 Å regardless of molecular conformation, while the interresidue H8–H1′ (H6–H1′) distances strongly depend on conformation (Wüthrich, 1986). The A H8-H1′ cross peaks were found in the most downfield region of the NOESY contour plot (Figure 6). The only H1′ proton that gave a cross peak to a single H8 proton was assigned to A20 H1′, and the H8 involved was assigned to A20 H8. In addition to this intraresidue cross peak, the A20 H8 gave another cross peak to an H1′ proton, which was assigned to the A19 H1′. Then the A19 H8 was assigned from the intraresidue H1′–H8 cross peak, and so on. Thus, the "walk-around" procedure for assigning DNA protons in antiparallel B-DNA helices (Scheek et al., 1983, 1984) is still applicable for this parallel-stranded DNA hairpin. Other regions of the NOESY spectra provided additional information for making sequential assignments. In the base proton–H3′ region (Figure 7), medium-intensity intraresidue H8-H3′ cross peaks were detected. The cross peaks for A20, A19, A18, A14, and A13 are well resolved. The three residues A15, A16, and A17 have very similar H8 and H3′ proton chemical shifts (Figure 7). Some resolved interresidue H8(*i*)–H3′(*i*–1) cross peaks were also observed, among them a weak cross peak between an A H8 and a C H3′ proton (Figure 7). From inspection of the sequence of the hairpin, these were assigned to residues A13 and C12, respectively. The distinction between the H2′ and H2″ could be made using NOESY spectra

Chart II: Sequence and Numbering Used for the d(T8()C4A8) Hairpin[a]

		C10 C11		
5′	C9		C12	
5′	T8	—	A13	
	T7	—	A14	
	T6	—	A15	
	T5	—	A16	
	T4	—	A17	
	T3	—	A18	
	T2	—	A19	
3′	T1	—	A20	3′

[a] The hydrogen bonding between the stem A and T residues is indicated by a dash.

recorded with short mixing times (data not shown); this is based on the fact that the distance between H1′ and H2″ is always smaller than the corresponding distance between H1′ and H2′ (Wüthrich, 1986). For the residues A13, A14, and A20, the H2″ proton is at an upfield chemical shift position from the H2′ proton. For A19, the reverse is true, while the H2′ and H2″ protons of residues A15–A18 display almost the same chemical shifts. Finally, the H2 protons of A20, A19, A17, A16, and A15 were assigned from weak intraresidue NOE cross peaks to their respective H1′ protons (Figure 6). This intraresidue NOE was not detected for residues A13, A14, and A18. The A H2 assignments were completed and checked for consistency by using the observed NOE peaks between neighboring A H2 protons (cf. Figure 2, which were recorded at 4 mM sample concentration to illustrate the multimer formation). The chemical shifts of the A H2 protons are about 0.3 ppm downfield from corresponding resonances in antiparallel structures.

The assignment of the T residues was accomplished in a similar manner. Starting from the T1 and T8 residues, sequential assignments were made via the interresidue H6-(i)–H1′(i+1) NOEs (here i+1 is at the 5′-end of residue i, see Chart II) and the H6(i)–H3′(i+1) NOEs. The four T residues in the middle (T3–T6) have almost identical base and sugar proton chemical shifts, indicating that their conformation is quite uniform.

The C9 residue was identified as stated above. The sequential assignments for the other C residues were obtained from the observed interresidue H6(i)–H3′(i–1) NOEs (Figure 7). The interresidue H6–H1′ NOEs for the C residues are either missing or very weak (Figure 6). The resonances of the H3′ and H2′,H2″ protons of the C residues are shifted upfield relative to those of the T and A residues. The assignments are summarized in Table I.

^{31}P Assignments of the Sugar–Phosphate Backbone. The ^{31}P resonances were assigned from a ^{1}H-detected ^{1}H–^{31}P correlation experiment (Figure 8). The most downfield ^{31}P signal did not give cross peaks to any of the H3′ protons and therefore was assigned to the 5′–P–5′ linkage between residues T8 and C9. The rest of the ^{31}P signals resonate within 0.5 ppm of each other; their assignments were obtained from the proton assignments. The resonances for the phosphorous linkages of the T-strand are upfield from those of the A residues; the ones for the C residues are located in between these. In addition to the H3′–P cross peaks, both the H4′–P and H5′,H5″–P cross peaks were observed.

The Molecular Conformation As Deduced from the NMR Data. Differences in sugar ring puckering will give rise to differences in ring proton coupling constants; consequently, the deoxyribose ring pucker can be estimated from the cross peak fine structure measured in a DQF-COSY spectrum. The H1′ proton resonance is characterized by a total splitting of $^{3}J_{H1'H2'} + {}^{3}J_{H1'H2''}$. The sum of these coupling constants can be measured from the separation of the outer peaks of resolved H1′–H2′ or H1′–H2″ cross peaks of the H1 multiplets along the F_2 dimension (cf. Figure 9). The measured $^{3}J_{H1'H2'} + {}^{3}J_{H1'H2''}$ values were 15.2–16.0 Hz for nearly all of the A residues. The chemical shifts of the H1′ protons of A15, A16, and A17 are almost identical, leading to signal overlap; in this case the measured splitting (16 Hz) only provides an upper limit. Unfortunately, the cross peak overlap is rather severe for the T residues, although it appears that the splitting values for the T1–T6 residues are in the same range (cf. Figure 9). These values for $^{3}J_{H1'H2'} + {}^{3}J_{H1'H2''}$ indicate that the sugar ring pucker of the stem residues are in the C2′-endo to C1′-exo range (Rinkel & Altona, 1987) (with the possible exception of A13, T7, and T8). The $^{3}J_{H1'H2'} + {}^{3}J_{H1'H2''}$ for loop residues C10 and C11 was measured as 16.0 and 15.0 Hz, respectively, indicating that their sugar ring pucker is not different from that of the stem residues. The H1′–H2′ and H1′–H2″ cross peaks for C9 were very weak, and those of C12 were not detected; the implications of this will be discussed below.

From an analysis of the cross peak fine structures and intensities (Figure 9), the following generalized information regarding the sugar proton coupling constants for all of the T and C residues was obtained: $^{3}J_{H1'H2'} > {}^{3}J_{H1'H2''}$, $^{3}J_{H3'H2'} > {}^{3}J_{H3'H2''}$. In addition, $^{3}J_{H3'H2''}$ is always very small (<2 Hz). The chemical shifts of the H2′ and H2″ protons of the majority of the A residues (A15–A18) are too close for an analysis of individual coupling constants. However, $^{3}J_{H1'H2'} > {}^{3}J_{H1'H2''}$ can be recognized for A19, A20, and A14, and $^{3}J_{H3'H2'} > {}^{3}J_{H3'H2''}$ in A20 (Figure 9). These coupling constants are consistent with sugar ring conformations in the C2′-endo to C1′-exo range (Rinkels & Altona, 1987).

Since the deoxyribose rings are in the C2′-endo and C1′-exo conformational range, the observed intraresidue NOESY cross peaks of H8(H6)–H3′ (Figure 7) and of H8(6)–H4′ (Figure 5) unambiguously identify that the base orientation is anti for these residues. With a syn orientation, these distances are beyond the NOE observable range; but with an anti orientation they can be <5 Å and should give rise to observable NOESY cross peaks (Wüthrich, 1986).

The proton chemical shifts of the A and T residues are generally comparable to those of corresponding protons in antiparallel-stranded B-type oligo-DNA duplexes. This indicates that a similar base stacking exists in this parallel-stranded stem and suggests the presence of a right-handed helix. The observed NOESY cross peaks between neighboring A H2 protons (Figure 2) provide further evidence for similar base stacking. Furthermore, the observed interresidue H8-(H6)-H1′ (5′-end neighbor) (Figure 6) and H8(H6)–H3′ (5′-end neighbor) (Figure 7) NOESY cross peaks suggest that the right-handedness continues throughout the whole stem. The chemical shifts of the H3′, H2′, and H2″ protons of the C residues (especially C10, C11, and C12) are relatively

Table I: Complete Proton NMR Assignment for d(T8()C4A8)[a]

	H8	H2	H6	H5	H1′	H3′	H4′	H5′	H5″	H2″	H2′	CH_3
T(1)			7.46		6.15	4.56	4.03	4.15	4.05	2.25	2.20	1.68
T(2)			7.48		6.05	4.90	4.20	4.14	4.05	2.52	2.23	1.72
T(3)			7.48		6.05	4.90	4.20	4.14	4.05	2.52	2.23	1.74
T(4)			7.50		6.08	4.90	4.20	4.14	4.05	2.52	2.23	1.74
T(5)			7.50		6.15	4.92	4.29	4.14	4.05	2.52	2.23	1.74
T(6)			7.54		6.15	4.92	4.29	4.14	4.05	2.52	2.23	1.74
T(7)			7.54		6.15	4.92	4.29	4.14	4.05	2.62	2.32	1.74
T(8)			7.48		6.13	4.90	4.20	4.14	4.05	2.60	2.30	1.80
C(9)			7.69	5.95	6.04	4.74	4.27	4.12	4.08	2.50	2.18	
C(10)			7.84	6.04	6.17	4.64	4.30	4.12	4.08	2.38	2.07	
C(11)			7.61	5.91	6.04	4.62	4.07	3.92	3.83	2.22	1.82	
C(12)			7.48	5.89	5.91	4.58	3.97	3.81	3.71	2.02	1.87	
A(13)	8.17	7.71			5.30	4.85	4.25	3.95	3.90	2.58	2.67	
A(14)	8.21	7.54			5.37	4.94	4.31	4.12	4.07	2.59	2.59	
A(15)	8.16	7.35			5.38	4.98	4.34	4.12	4.07	2.59	2.59	
A(16)	8.14	7.25			5.39	4.98	4.34	4.12	4.07	2.59	2.59	
A(17)	8.14	7.25			5.39	4.98	4.34	4.12	4.07	2.59	2.59	
A(18)	8.09	7.31			5.47	4.97	4.34	4.12	4.07	2.57	2.57	
A(19)	7.99	7.39			5.72	4.97	4.35	4.12	4.07	2.61	2.52	
A(20)	8.09	7.74			6.18	4.68	4.20	4.12	4.07	2.60	2.35	

[a] All chemical shifts are reported in parts per million with respect to DSS.

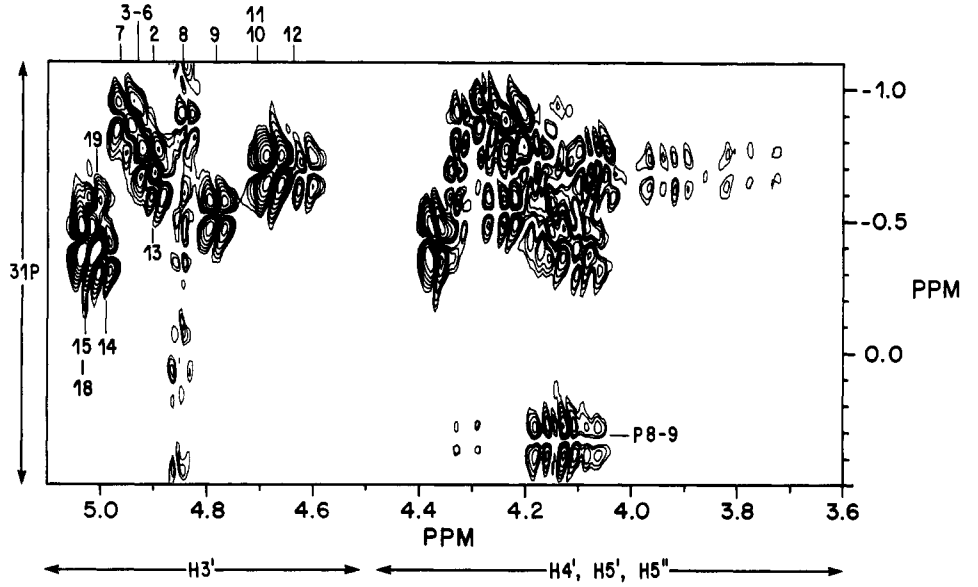

FIGURE 8: Contour plot of a pure absorption-mode proton-detected 2D ^1H–^{31}P correlation spectrum of d(T8()C4A8). The positions of the H3′ protons are labeled with the appropriate residue numbers. The most downfield ^{31}P resonance was assigned to P_{8-9}, which does not show a cross peak to any H3′ proton. Both positive and negative contour levels are plotted. The ridge at ~4.87 ppm is from residual water. Other details are given under Materials and Methods.

upfield-shifted, indicating altered base stacking in these residues.

The measured ^{31}P chemical shifts are plotted against the sequence in Figure 10. On both strands, the four phosphates in the middle of the stem have virtually the same chemical shifts. The phosphate groups between the A residues display a chemical shift which is about 0.3 ppm upfiled from the shifts for the T residues. It suggests that the backbone disturbance caused by the C4 loop or by the 5′–P–5′ linkage is felt up to three residues from the junction, but not farther into the stem. Phosphorus chemical shifts in DNA have been shown to correlate with the backbone torsion angles ϵ and ζ (Powers et al., 1989, 1990). A more upfield ^{31}P chemical shift is related to the lower energy BI conformations (Dickerson, 1983). A higher energy BII conformation is characterized by a more downfield chemical shift. Using the ^{31}P chemical shifts estimated for the pure BI and BII conformation (Roongta, 1990), we show that both of the strands in our hairpin are mainly in the BI conformation. If we assume that a fast equilibrium between BI and BII conformers exists and that this gives rise to the averaged ^{31}P chemical shifts, then the T strand has a higher BI population (82%), while the A strand is about 65% in BI.

The chemical shifts of the phosphorus groups in the C4 loop are quite uniform (Figure 10). This suggests that there are no abrupt turns in the backbone structure in the loop. The P_{8-9} resonance for the 5′–P–5′ linkage is downfield from the other resonances. However, due to the lack of available model compounds, it is not directly clear how its shift relates to backbone torsion angles.

The width of the H3′ multiplet in the oligodeoxynucleotides is determined by $^3J_{H3'H2'} + {}^3J_{H3'H2''} + {}^3J_{H3'H4'} + {}^3J_{H3'P}$. Phosphorus decoupling should therefore reduce the width of the H3′ multiplet. The heteronuclear coupling constants $^3J_{H3'P}$ can thus be estimated by comparing the extent of the outer splitting of the H3′ proton multiplets in a high-resolution (1 Hz/point) proton DQF-COSY experiment and in a ^{31}P-decoupled proton DQF-COSY experiment. Only the H3′ protons of the loop C residues and the T8 were resolved well enough to allow the assessment (C12, 5.6 Hz; C11, 4.3 Hz;

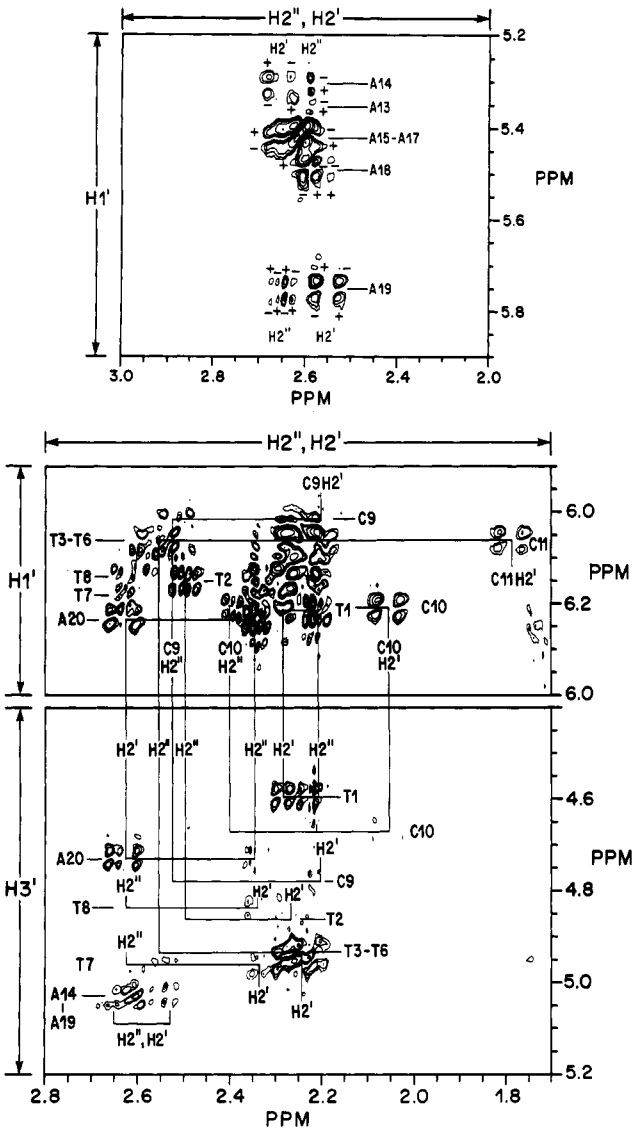

FIGURE 9: Regions of a 500-MHz DQF-COSY spectrum of D(T8()C4A8) showing cross peaks between the H1′ and the H2′, H2″ and between the H3′ and the H2′, H2″ protons. Both positive and negative contour levels are plotted; they are indicated by + and − signs, respectively, in the top part, but they are not distinguished in the bottom part.

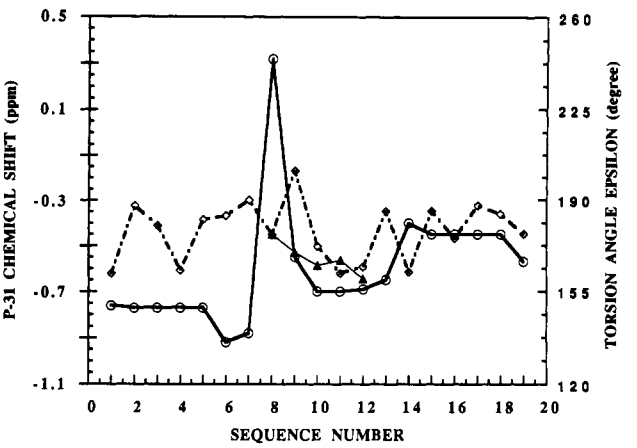

FIGURE 10: ^{31}P chemical shifts (○) of d(T8()C4A8) vs their position along the sequence. Also plotted are the backbone torsion angles ϵ of the residues 8–12 (▲) estimated from the $J_{P-H3'}$ coupling. The bond angles measured in the model (◇) are also indicated for comparison.

C10, 5.0 Hz; C9, 3.8 Hz; T8, 2.8 Hz). The torsion angles ϵ for these residues were derived using a ^{1}H–^{31}P Karplus relationship ($^3J = 15.3 \cos^2\theta - 6.1 \cos\theta + 1.6$) (Lankhorst et al., 1984) and $\epsilon = -\theta - 120°$ (Powers et al., 1990). Four possible ϵ values correspond to each ^3J value measured; if we choose the one inside the range of the ϵ values in B-DNA, the torsion angles ϵ of the residues C12, C11, C10, C9, and T8 are 160°, 167°, 165°, 170°, and 177°, respectively. These ϵ angles are plotted together with the ^{31}P chemical shifts in Figure 10. In the ^{31}P-decoupled DQF-COSY, some cancellation of the antiphase doublet is likely (data not shown). Therefore, the measured splittings (9.4–11.0 Hz) provide an underestimation of the true splitting, and as a result the calculated $^3J_{H3'P}$ represents an upper limit.

The loop and the loop–stem junctions display some unusual behaviors. In the DQF-COSY spectrum, the H1′–H2′, H1′–H2″ cross peaks of residue C12 were noticeably missing; those of A13 were very weak (Figure 9). Apparently, cross peak cancellation occurs because of broader signals which could be due to an intermediate exchange process involving these protons. The NOE cross peaks between the H1′ and H2′ and between the H1′ and the H2″ of C12, as well as A13, were detected but are of lower intensity (data not shown). This is again consistent with the existence of a conformational exchange process involving the H1′ resonances (since the H3′–H2′ and the H3′–H2″ NOE cross peaks of these two residues are of a more normal intensity) reducing the correlation times and thus the NOE intensities. The same effects were observed for C9, T8, and T7 but to a lesser extent. This implies that the junction residues show somewhat more mobility. The loop residues C10 and C11 are characterized by normal COSY and NOESY cross peaks, which suggests that they are in a stable conformation. Cross peaks indicating base stacking were observed for these two loop bases.

NOE-Restrained Energy Minimization. A starting model for the d(T8()C4A8) hairpin was built using standard B-DNA coordinates as described under Materials and Methods. In this model, the A and T bases are held together with reverse Watson–Crick base pairing (Saenger, 1984), and each strand is like B-DNA with a C2′-end sugar conformation and an anti base orientation for each nucleotide. This is consistent with the NMR parameters analyzed above. To refine this model, a total number of 336 proton NOEs (see Table II) were converted into approximate distance constraints (see Materials and Methods). The A H2 protons normally form a relaxation network together with the solvent-exchangeable imino and amino protons, while the rest of the nonexchangeable protons form another relaxation network with limited interactions between the two networks (Boelens et al., 1985). We observed that for each A H2 proton, the cross peak intensities were less than 5% of the diagonal peak intensity at all mixing times. Recording NOESY experiments with longer delays between consecutive scans would have better defined the intensities of the cross peaks involving the A H2 protons. However, all these cross peaks are "weak", the distances involving the A H2 are modeled between 2 and 5 Å and hence this should have little influence on the final structure. Constraints for hydrogen bonding were also included in the energy minimization. The number of NOE distance violations in the starting structure was small (total 15, of which 3 were from the A residues and 6 each were from the T residues and the loop C residues, respectively). Only one starting model was used. In the energy-minimized structure (Figure 11), one violation larger than 0.1 Å remained which was in residue A19. The rmsd between the corresponding distances and the NOE constraints was 0.012. The equal width of the two grooves thus appears to be mainly the result of the reverse

Table II: Proton NOE Data of d(T8⟨⟩C4A8) Used in the Restrained Energy Minimization[a,b,c]

	intraresidue															
residue no.	H6/H8 | H1′	H6/H8 | H2′	H6/H8 | H2″	H6/H8 | H3′	H6/H8 | H4′	H1′ | H2′	H1′ | H2″	H1′ | H3′	H1′ | H4′	H3′ | H2′	H3′ | H2″	H3′ | H4′	H4′ | H2′	H4′ | H2″	H5 | H2′	H2 | H1′
1	+	+++	+	+	+	+	+	+	+	+++	+++	++	+	+		
2	+	++	+	+	+	+	+++	+	+	+++	+++	++	+	+		
3–6	+	+++	+	+	+	+	+++	+	++	+++	+++	++	+	+		
7	+	+++	+	+	+	+	+++	+	+	+++	+++	++	+	+		
8	+	+++	+	+	+	+	+++	+	++	+++	+++	++	+	+		
9	+	+++	+	+	+	+	+++	+	+	+++	+++	++	+	+		
10	+	+++	+	+	+	+	+++	+	+	+++	+++	++	+	+	+	
11	+	+++	+	+	+	+	+++	+	+	+++	+++	++	+	+		
12	+	+++	+	+	+	+	+	+	+	+++	+++	++	+	+		
13	+	+++	+	+	+	+	++	+		+++	+++	++	+	+		
14	+	+++	+	+	+	+	+++	+	+	+++	+++	++	+	+		+
15–18	+	+++	+	+	+	+	+++	+	++	+++	+++	++	+	+		+
19	+	+++	+	+	+	+	+++	+	+	+++	+++	++	+	+		+
20	+	+++	+	+	+	+	+++	+	++	+++	+++	++	+	+		+

residue no. (*i*)	H6/H8 | H1′	H6/H8 | H2″	H6/H8 | H3′	H6 | H5′/H5″	H2–H2
		interresidue [(*i*) – (*i* + 1)]			
1	+	+	+		
2	+	+	+		
3–6	+	+	+		
7	+	+	+		
8					
		interresidue [(*i*) – (*i* – 1)]			
9				+	
10			+		
11		+			
12		+			
13					
14	+	+	+		
15–18	+	+	+		+
19	+	+			+
20	+	+	+		

[a] The symbols +, ++, and +++ indicate weak, medium, and strong NOEs observed between the corresponding protons, respectively. [b] A total of 403 NOEs were identified, but only 336 were used for the calculations (see Materials and Methods). [c] Because of the repetitive polymeric nature of the hairpin stem, the intensities for overlapping cross peaks for the parallel A·T stem were estimated by assuming equal cross peak intensities and/or by comparison to a resolved cross peak of the same type.

Watson–Crick base pairing, and the stem of our refined hairpin structure is rather similar to previously proposed parallel-stranded models (Pattabiraman, 1986; van de Sande et al., 1988).

The hydrogen-bonding energy in the refined model is comparable to that of Watson–Crick base pairing in anti-parallel B-DNA. Likewise, the base-stacking energy for the stem residues is also close to that found in B-DNA. This is consistent with the idea that they are energetically about equally stable (Pattabiraman, 1986). The helix diameter is ~20 Å with a rise of 9.4 residues/turn. Interestingly, the two grooves of the helix are now of similar width (Figure 11). The average center–center distance between the closest phosphorus atoms across the "major" groove is 13.0 Å; across the "minor" groove this distance is 16.0 Å. The corresponding numbers are 17.4 and 11.5 Å, respectively, for the major and minor grooves in an antiparallel B-DNA helix. This gives the parallel-stranded structure a very different accessible surface and a different combination of exposed base groups in the two grooves. The deoxyribose ring conformation for most of the residues in the refined model is in the C2′-endo to C1′-exo range; this is consistent with the analysis from the DQF-COSY spectrum. Yet, the C12, A13, and two T residues display a sugar ring pucker closer to C3′-endo conformation. In Figure 12, the backbone torsion angles ϵ and ζ measured from the model are plotted. As noted above, the angles of all the residues are close to the BI conformation region, although the values for the A residues in the model are somewhat more toward the BII conformation. We conclude that the refined model represents the predominant low-energy conformer, which is in equilibrium with a small amount (<20%) of conformers in which both strands can be in the BII area; this interpretation provides a satisfactory explanation for all the NMR data. The C9 residue, as well as the T7 and T8 residues, show somewhat smaller ζ angles. The ϵ of the C9 is smaller than the value estimated from the ^1H–^{31}P coupling constant (–190°), while the ϵ for T8, C10, C11, and C12 compares favorably with the value estimated from the phosphorus proton couplings (Figure 10). These small differences can be caused by coupling constant averaging and experimental inaccuracy.

CONCLUSIONS

Parallel-stranded DNA can form in duplexes of homo-oligomeric or alternating dA·T tracts of DNA (Germann et al., 1988; Ramsing & Jovin, 1988). Unfortunately, these structures are relatively unstable and do not lend themselves readily to a complete structural analysis by 2D NMR at this stage. Much greater thermodynamic stability of parallel-stranded DNA has been obtained by synthesizing DNA hairpins with an unusual 5′–5′ or 3′-3′ phosphodiester linkage in the loop; this gives the strands the same polarity (van de

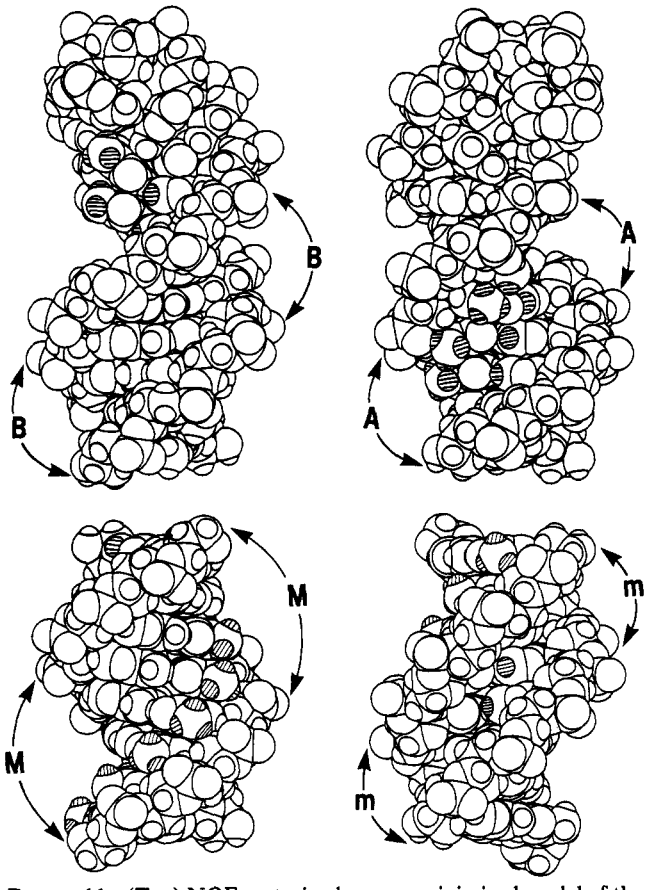

FIGURE 11: (Top) NOE-restrained energy-minimized model of the parallel-stranded hairpin d(T8⟨⟩C4A8). The views shown in the two panels are related by rotation of 180° around the helix axis; the two different grooves are indicated as A and B. (Bottom) B-DNA model of a T8–A8 duplex. The major and minor (indicated as "M" and "m", respectively) grooves are shown in the two panels. The A H2 and the T methyl protons on each strand are marked by hatched lines.

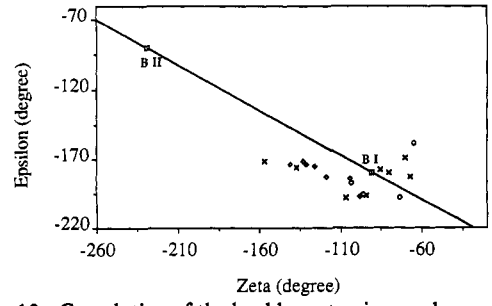

FIGURE 12: Correlation of the backbone torsion angle ϵ and ζ of the refined model. The straight line represents the best linear correlation ($\zeta = -367.5 - 1.54\epsilon$) obtained from crystallographic B-DNA structures (Powers et al., 1990). The angles for BI and BII conformation are represented by □ on the line as indicated. The ϵ values correspond to the values used in the Karplus equation (see text) and in Figure 10 after adding 360. (×, T residues; ◇, A residues; ○, C residues).

Sande et al., 1988). The unusual phosphodiester linkage simply serves to stabilize intramolecular parallel-stranded DNA formation. In this work we have studied the hairpin d(T8⟨⟩C4A8) which can form a homooligomeric parallel-stranded stem (Germann et al., 1989). The polymeric nature of the stem caused signal overlap in our 2D spectra, which complicated the NMR analysis to some extent. However, this could not be avoided, as alterations in the stem sequences would have destabilized the structure.

We have found that the sugar–phosphate backbone in the parallel-stranded stem of the hairpin is almost identical to that observed in regular B–DNA; this is consistent with the model proposed originally by Pattabiraman (1986). The helix is right-handed, which is consistent with the outcome of CD experiments (Germann et al., 1989). On the basis of the detection of unusual interstrand NOE interactions between the A H2 and the T methyl groups, we have shown that reverse Watson–Crick base pairs are formed; this notion is in agreement with earlier studies (Pattabiraman, 1986; Germann et al., 1989; Otto et al., 1991). This 180° flip of the T residue, when compared to Watson–Crick base pairs, places the A H2 and the T methyl group in the same groove (Chart I and Figure 11). The most striking feature of the NOE-restrained structure is the nearly equal width of the two grooves. This feature explains why drugs that are specific for the minor groove, such as Hoechst 33258, bind poorly to parallel-stranded DNA (van de Sande et al., 1988; Germann et al., 1989). Finally, it should be noted that the structure determined here for a parallel-stranded DNA comprising normal oligonucleotides is quite distinct from the parallel-stranded structure formed by the association of the unnatural α-deoxyoligonucleotides with its complementary β oligonucleotide sequence (Lancelot et al., 1989; Guesnet et al., 1990).

ACKNOWLEDGMENT

We are indebted to S. Stauffer and J. Cleland for the typing of the manuscript.

REFERENCES

Arnott, S., & Hukins, D. W. L. (1972) *Biochem. Biophys. Res. Commun. 47*, 1504–1510.

Bax, A. (1989) *Annu. Rev. Biochem. 58*, 223–256.

Bax, A., & Davis, D. G. (1985) *J. Magn. Reson. 65*, 355–360.

Blommers, M. J. J., van de Ven, F. J. M., van der Marel, G. A., van Boom, J. H., & Hilbers, C. W. (1991) *Eur. J. Biochem. 201*, 33–51.

Boelens, R.; Scheek, R. M., Dijkstra, K., & Kaptein, R. (1985) *J. Magn. Reson. 62*, 378–386.

Braunsch, W. L., & Ernst, R. R. (1983) *J. Magn. Reson. 53*, 521–528.

Brooks, B. R.; Bruccoleri, R. E.; Olafson, B. D., States, D. J., Swaminathan, S., & Karplus, M. (1983) *J. Comput. Chem. 4*, 187–217.

Cohen, J. S. (1987) *Trends Biochem. Sci. 12*, 133–135.

Dickerson, R. E. (1983) *J. Mol. Biol. 166*, 419–441.

Germann, M. W., Kalisch, B. W., & van de Sande, J. H. (1988) *Biochemistry 27*, 8302–8306.

Germann, M. W., Vogel, H. J., Pon, R. T., & van de Sande, J. H. (1989) *Biochemistry 28*, 6220–6228.

Germann, M. W., Kalisch, B. W., Pon, R. T., & van de Sande, J. H. (1990) *Biochemistry 29*, 9426–9432.

Guesnet, J.-L., Vovelle, F., Thuong, N. T., & Lancelot, G. (1990) *Biochemistry 29*, 4982–4991.

Koole, L. H., van Genderen, M. H. P., & Buck, H. M. (1987) *J. Am. Chem. Soc. 109*, 3916–3921.

Lancelot, G., Guesnet, J.-L., & Vovelle, F. (1989) *Biochemistry 28*, 7871–7878.

Lankhorst, P. P., Haasnoot, C. A. G., Erkelens, C., & Altona, C. (1984) *J. Biomol. Struct. Dyn. 1*, 1387–1405.

Macura, S., Huang, Y., Suter, D., & Ernst, R. R. (1981) *J. Magn. Reson. 43*, 259–281.

Marion, D., & Wüthrich, K. (1983) *Biochem. Biophys. Res. Commun. 113*, 967–974.

Morvan, F., Rayner, B., Imbach, J. L., Lee, M., Hartley, J. A., Chang, D. K., & Lown, J. W. (1987) *Nucleic Acids Res. 15*, 7027–7044.

Nilsson, L., & Karplus, M. (1986) *J. Comput. Chem. 7*, 691–716.

Otto, C., Thomas, G. A., Rippe, K., Jovin, T. M., & Peticolas, W. L. (1991) *Biochemistry 30*, 3062–3069.
Pattabiraman, N. (1986) *Biopolymers 25*, 1603–1606.
Powell, M. J. D. (1977) *Math. Program. 12*, 241–254.
Powers, R., Olsen, R. K., & Gorenstein, D. G. (1989) *J. Biomol. Struct. Dyn. 7*, 515–556.
Powers, R., Jones, C. R., & Gorenstein, D. G. (1990) *J. Biomol. Struct. Dyn. 8*, 253–294.
Praseuth, D., Chassignol, M., Takasugi, M., Le Doan, T., Thuong, N. T., & Helene, C. (1987) *J. Mol. Biol. 196*, 939–942.
Quaedflieg, P. J. L. M., van der Heiden, A. P., Koole, L. H., van Genderen, M. H. P., & Buck, H. M. (1990) *J. Org. Chem. 55*, 122–127.
Ramsing, N. B., & Jovin, T. M. (1988) *Nucleic Acids Res. 14*, 6659–6676.
Ramsing, N. B., Rippe, K., & Jovin, T. M. (1989) *Biochemistry 28*, 9528–9535.
Rance, M., Sorensen, O. W., Bodenhausen, G., Wagner, G., Ernst, R. R., & Wüthrich, K. (1983) *Biochem. Biophys. Res. Commun. 117*, 479–485.
Rinkel, L. B., & Altona, C. (1987) *J. Biomol. Struct. Dyn. 4*, 621–649.
Rippe, K., Ramsing, N. B., & Jovin, T. M. (1989) *Biochemistry 28*, 9536–9541.
Roongta, V. A., Jones, C. R., & Gorenstein, D. G. (1990) *Biochemistry 29*, 5245–5258.
Saenger, W. (1984) *Principles of Nucleic Acid Structure*, Springer-Verlag, New York.
Sarma, M. H., Gupta, G., & Sarma, R. H. (1986) *FEBS Lett. 205*, 223–229.
Scheek, R. M., Russo, N., Boelens, R., & Kaptein, R. (1983) *J. Am. Chem. Soc. 105*, 2914–2916.
Scheek, R. M., Boelens, R., Russo, N., van Boom, J. H., & Kaptein, R. (1984) *Biochemistry 23*, 1371–1376.
Sklenar, V., Miyashiro, H., Zon, G., Miles, T., & Bax, A. (1986) *FEBS Lett. 208*, 94–98.
Singh, U. C., Weiner, P. K., Caldwell, J. W., & Kollman, P. A. (1988) *AMBER3.0, Assisted Model Building with Energy Refinement*, Department of Pharmaceutical Chemistry, University of California, San Francisco.
Thuong, N. T., Asseline, U., Roig, V., Takasugi, M., & Helene, C. (1987) *Proc. Natl. Acad. Sci. U.S.A. 84*, 5129–5133.
van de Sande, J. H., Ramsing, N. B., Germann, M. W., Elhorst, W., Kalisch, B. W., Kitzing, E. V., Pon, R. T., Clegg, R. C., & Jovin, T. M. (1988) *Science 241*, 551–557.
van de Ven, F. J. M., & Hilbers, C. W. (1988) *Eur. J. Biochem. 178*, 1–38.
van Genderen, M. H. P., Hilbers, M. P., Koole, L. H., & Buck, H. M. (1990) *Biochemistry 29*, 7838–7845.
Wang, K. Y., Borer, P. N., Levy, G. C., & Pelczer, I. (1992) *J. Magn. Reson. 96*, 165–170.
Wüthrich, K. (1986) *NMR of Proteins and Nucleic Acids*, John Wiley & Sons, Inc., New York.
Zhou, N., & Vogel, H. J. (1993) *Biochemistry* (preceding paper in this issue).